BIOCHEMISTRY
including biophysical chemistry & molecular biology

Article

pubs.acs.org/biochemistry

Hydrodynamic and Functional Analysis of HIV-1 Vif Oligomerization

Stephen M. Techtmann,[†] Rodolfo Ghirlando,[‡] Sandra Kao,[§] Klaus Strebel,[§] and Ernest L. Maynard*[,†]

[†]Department of Biochemistry and Molecular Biology, Uniformed Services University of the Health Sciences, Bethesda, Maryland 20814, United States

[‡]Laboratory of Molecular Biology, National Institute of Diabetes and Digestive and Kidney Diseases, National Institutes of Health, Bethesda, Maryland 20892, United States

[§]Laboratory of Molecular Microbiology, National Institute of Allergy and Infectious Diseases, National Institutes of Health, Bethesda, Maryland 20892, United States

S *Supporting Information*

ABSTRACT: HIV-1 Vif is an accessory protein that induces the proteasomal degradation of the host restriction factor, apolipoprotein B mRNA-editing enzyme catalytic polypeptide-like 3G (APOBEC3G). The N-terminal half of Vif binds to APOBEC3G, and the C-terminal half binds to subunits of a cullin 5-based ubiquitin ligase. This Vif-directed ubiquitin ligase induces the degradation of APOBEC3G (a cytidine deaminase) and thereby protects the viral genome from mutation. A conserved PPLP motif near the C-terminus of Vif is essential for Vif function and is also involved in Vif oligomerization. However, the mechanism and functional significance of Vif oligomerization is unclear. We employed analytical ultracentrifugation to examine the oligomeric properties of Vif in solution. Contrary to previous reports, we find that Vif oligomerization does not require the conserved PPLP motif. Instead, our data suggest a more complex mechanism involving interactions among the HCCH motif, the BC box, and downstream residues in Vif. Mutation of residues near the PPLP motif (S165 and V166) affected the oligomeric properties of Vif and weakened the ability of Vif to bind and induce the degradation of APOBEC3G. We propose that Vif oligomerization may represent a mechanism for regulating interactions with APOBEC3G.

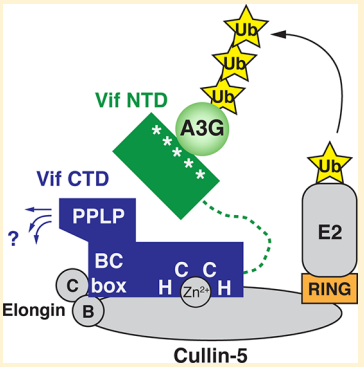

HIV-1 virion infectivity factor (Vif) is an accessory protein that is required for viral replication in T-cells. Such "non-permissive" cells restrict the replication of *vif*-deficient HIV-1 because they express apolipoprotein B mRNA-editing enzyme catalytic polypeptide-like 3G (APOBEC3G)[1] as well as the closely related APOBEC3F.[2−5] APOBEC3G contains two copies of the cytidine deaminase (CDA) domain. The N-terminal CDA domain mediates packaging of APOBEC3G into virus particles[6] by a process that involves interactions with the nucleocapsid domain of Gag.[6−15] APOBEC3G is delivered in the virus particle to the target cell where it catalyzes the deamination of cytidines in the minus strand DNA produced by viral reverse transcription. The resulting C-to-U mutations are copied into the plus strand DNA as G-to-A mutations that block viral replication.[2−5,16−20] Vif prevents the encapsidation of APOBEC3G into virus particles. Vif functions as an adaptor protein that binds to APOBEC3G and to subunits of a RING-cullin ubiquitin ligase, including elongin B/C and cullin 5 (Cul5).[21] This complex, which includes the recently identified T-cell differentiation factor CBF-β,[22,23] induces the polyubiquitination and proteasomal degradation of APOBEC3G.[21,24−28]

HIV-1 Vif is a 23 kDa protein of 192 amino acids. APOBEC3G binds to a surface in Vif formed by a nonlinear array of sequence motifs that span residues 14−89.[29−35] Elongin B/C binds to the conserved BC box motif in Vif (S^{144}LQYLALAAL^{153}).[36,37] Two regions in Vif appear to be important for binding to Cul5. The HCCH motif ($H^{108}C^{114}C^{133}H^{139}$) is required for interaction with Cul5.[38−41] Zinc binds specifically and reversibly to the HCCH motif to generate a conformation capable of mediating protein−protein interactions.[42] An HCCH-containing fragment of Vif (residues 101−141) interacts directly with Cul5 in a zinc-dependent manner, suggesting that zinc modulates the conformation of Vif to expose a Cul5 binding site.[41] The P^{161}PLP^{164} motif located downstream from the BC box has also been implicated in Cul5 binding[43,44] and bears sequence similarity to the cullin box motif that is conserved in suppressor of cytokine signaling (SOCS) proteins.[45] However, the PPLP motif appears to play a minor thermodynamic role in forming the Vif−Cul5−elongin BC complex, which is driven by the high (nanomolar) affinity of the BC box for elongin B/C.[44] A recent nuclear magnetic resonance (NMR) study demonstrated that the PPLP motif binds to elongin B,[46] and other studies suggest that the PPLP motif is required for APOBEC3G binding and degradation.[47,48] The PPLP motif is located in a region of Vif that is highly dynamic in solution.[49,50] Flexibility may allow this region of Vif to engage in diverse protein−protein interactions.

Received: November 22, 2011
Revised: February 27, 2012
Published: February 27, 2012

The ability of Vif to form diverse protein−protein interactions is further exemplified by the discovery that Vif forms homo-oligomers. Using a pull-down assay with GST-bound Vif and ^{35}S-labeled Vif, the region in HIV-1 Vif required for oligomerization was mapped to residues 151−164, which contains the conserved $P^{161}PLP^{164}$ motif.[51] Deletion of the PPLP motif inhibited the interaction between GST-bound Vif and ^{35}S-labeled Vif, and peptides containing the PPLP motif suppressed viral infectivity, suggesting that the PPLP motif is essential for the oligomerization and function of HIV-1 Vif.[52] Virus particles produced from cells treated with peptide antagonists of HIV-1 Vif oligomerization contained elevated amounts of APOBEC3G, further suggesting that oligomerization is critical for Vif function.[53] Despite the progress that has been made, a clear mechanistic understanding of Vif oligomerization is lacking. Toward this goal, we have employed analytical ultracentrifugation (AUC) to examine the oligomeric properties of Vif. These studies are complemented by functional assays to gauge the impact of mutations that affect the oligomeric state of Vif on the ability to bind to and induce the degradation of APOBEC3G.

MATERIALS AND METHODS

Cloning, Protein Expression, and Purification. Vif fragments were cloned into the pMal c-5x vector (NEB) using EcoRI and SbfI sites. Site-directed mutagenesis was performed using the QuikChange II XL mutagenesis kit (Agilent Technologies). Constructs were transformed into BL21(DE3) *Escherichia coli* cells. Bacteria were cultured in 2YT broth containing ampicillin and 1% glucose at 37 °C until the OD_{600} reached 0.6. Protein expression was induced with 0.5 mM IPTG and allowed to occur for 16 h at 18 °C. Cells were harvested by centrifugation at 5500*g* and 4 °C.

Cells were resuspended in buffer A [20 mM HEPES (pH 7.5), 150 mM NaCl, and 200 μM TCEP] supplemented with RNase/DNase and protease inhibitor (Roche Applied Sciences) and lysed in a French pressure cell. Lysates were clarified by centrifugation at 18000*g* and 4 °C for 30 min. The supernatant was allowed to incubate with amylose resin for 1 h at 4 °C, and the resin was washed with 5 column volumes of buffer A, followed by 5 column volumes of buffer B [20 mM HEPES (pH 8.0), 20 mM NaCl, and 200 μM TCEP]. Proteins were eluted with 2 column volumes of buffer B with 10 mM maltose. Vif-containing fractions were loaded onto a Resource Q column (GE Healthcare) equilibrated with buffer B. After being washed with buffer B, the protein was eluted with a linear gradient from 20 mM to 1 M NaCl over 10 column volumes. Vif was further purified with a Superose 6 column equilibrated in buffer A at a flow rate of 0.5 mL/min. Protein concentrations were determined by either a Bradford assay (Bio-Rad) using bovine serum albumin as a standard or the method of Edelhoch as described by Pace et al.[54]

Analytical Ultracentrifugation. Sedimentation velocity experiments were conducted at 20.0 °C on a Beckman Coulter Proteome XL-A or XL-I analytical ultracentrifuge using the absorbance optical detection system. Samples were loaded into two-channel, 12 mm path length sector-shaped cells (400 μL). Scans were acquired at 4 min intervals and rotor speeds of 45000 rpm; absorbance data were collected as single absorbance measurements at either 280 or 250 nm using a radial spacing of 0.003 cm.

Data were analyzed in SEDFIT 11.9b[55] in terms of a continuous $c(s)$ distribution. Solution densities (ρ) and viscosities (η) were calculated using SEDNTERP 1.2,[56] as were values of the partial specific volume (ν) of the protein. The $c(s)$ analyses were conducted using an s range of 0−25 with a linear resolution of 200 and maximal entropy regularization confidence levels (F ratio) of 0.68. In all cases, excellent fits were observed with root-mean-square deviations ranging from 0.0030 to 0.0091 absorbance unit. Sedimentation coefficients were corrected to standard conditions at 20.0 °C in water, $s_{20,w}$. Weight-average sedimentation coefficients, combining contributions from the monomer and oligomer, were obtained from the integral of the $c(s)$ distributions. These were used to construct weight-average sedimentation coefficient isotherms for the absorbance data.

Preparation of Vif(155−176) (PPLP peptide) and Analysis by CD Spectroscopy. HIV-1 Vif residues 155−176 (TPKKIKPPLPSVTKLTEDRWNK) were synthesized by solid phase peptide synthesis using Fmoc protection (Peptide 2.0, Chantilly, VA). Crude peptides were solubilized and purified by reverse phase high-performance liquid chromatography (HPLC) as previously described.[42] The peptide was dissolved in buffer A, and concentrations were determined using the method of Edelhoch as described by Pace et al.[54]

Peptide samples for far-UV CD spectroscopy were diluted to 48 μM in 10 mM MOPS (pH 7.4), 20 mM NaCl, and 40 μM TCEP. Solutions were placed in quartz cuvettes with path lengths of 1 mm, and far-UV CD spectra were recorded using a JASCO J-815 spectrometer at a scan speed of 20 nm/min and a bandwidth of 1 nm. Each spectrum represents the average of five successive baseline-corrected scans. The sample temperature for all CD measurements was maintained at 20 °C.

The mean residue molar ellipticity, $[\theta]$, was calculated according to the equation $[\theta] = (\theta \times MR)/(10lc)$, where θ is the measured ellipticity in millidegrees, MR is the mean residue mass (molecular weight of the peptide divided by the number of amino acid residues), l is the optical path length in centimeters, and c is the protein concentration in milligrams per milliliter. Spectral deconvolution was performed using the Contin algorithm[57] using reference set SP175[58] from the suite of programs available at the online server DICHROWEB (http://www.cryst.bbk.ac.uk/cdweb).[59,60]

APOBEC3G Degradation Assay. HeLa cells were transfected with pcDNA-APOBEC3G (0.5 μg) and pNL-A1-Vif constructs (4.5 μg). Cells were harvested 24 h later, and whole cell lysates were subjected to immunoblotting using antibodies to APOBEC3G or Vif. The APOBEC3G blot was subsequently reprobed with an antibody to tubulin, which served as a loading control.

Vif-APOBEC3G Co-Immunoprecipitation. HeLa cells were transfected with pcDNA-APOBEC3G-Myc (2 μg), pNL-A1-Vif (2 μg), and dominant negative Cul5[21] (Cul5ΔRbx, 1 μg). Cul5ΔRbx was included to prevent Vif-induced A3G degradation in this experiment. Cells were harvested 24 h later, lysed in CHAPS/DOC lysis buffer, and immunoprecipitated with a Myc-specific polyclonal antibody. Immunoprecipitates were separated by sodium dodecyl sulfate−polyacrylamide gel electrophoresis (SDS−PAGE) and probed with monoclonal antibodies to Vif and Myc. Amounts of wild-type (wt) Vif were defined as 100%. Amounts of coprecipitated mutant Vif proteins are expressed as percentage of wt Vif. Vif values were corrected for fluctuations in the APOBEC3G pull down.

dx.doi.org/10.1021/bi201738a | *Biochemistry* 2012, 51, 2078−2086

RESULTS

Full-length Vif is prone to aggregation,[42] and previous studies have indicated that the Vif C-terminal PPLP motif is responsible for oligomerization.[51,61] To avoid complications involving the Vif N-terminal domain (Vif residues 1−100), a domain that has a high affinity for nucleic acids,[62,63] we chose to focus on Vif C-terminal fragments (Vif residues 101−x). Several truncations were made in the C-terminus of Vif to highlight the regions involved in oligomerization and to assess the importance of the PPLP motif in oligomerization (Figure 1a). Vif fragments were expressed and purified as fusions to the

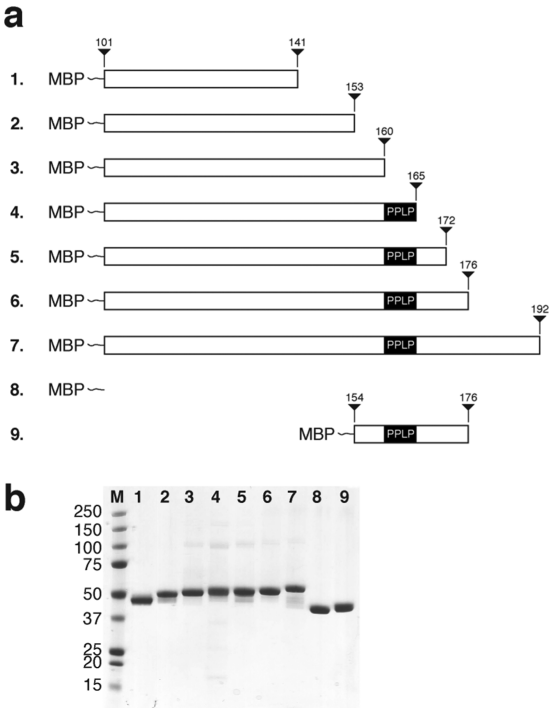

Figure 1. (a) Constructs used in this study. (b) SDS−PAGE of protein constructs. Purified proteins were boiled in reducing SDS sample buffer, separated on a 4 to 12% gel, and visualized by being stained with Colloidal Blue. Molecular mass standards are shown in kilodaltons.

maltose binding protein (MBP). MBP fusion results in high levels of expression in *E. coli* and facilitates rapid protein purification, and MBP is monomeric in solution. Figure 1b demonstrates the purity of the MBP fusion constructs used in this study.

Sedimentation $c(s)$ profiles for MBP-Vif(101−192), MBP-Vif(101−176), and MBP, presented in Figure 2, reveal that the MBP-Vif fragments are highly oligomeric and that MBP is almost completely monomeric. The $c(s)$ plot for MBP did reveal a small peak at 5.8 S, consistent with a dimer, accounting for ∼10% of the total protein. MBP used in this study contained the vector-derived sequence NAAAEFPAGN, which could promote nonspecific dimerization. In support of this, when MBP was cloned and expressed without these additional amino acids, AUC revealed that the protein is monomeric at high concentrations.[64] The species observed around $s_{20,w}$ = 3.8 S (44 kDa) have estimated molecular masses in close agreement with the calculated molecular masses of monomeric MBP-Vif(101−176) (50 kDa) and MBP-Vif(101−192) (52 kDa). We note that the $c(s)$ analysis involves direct boundary

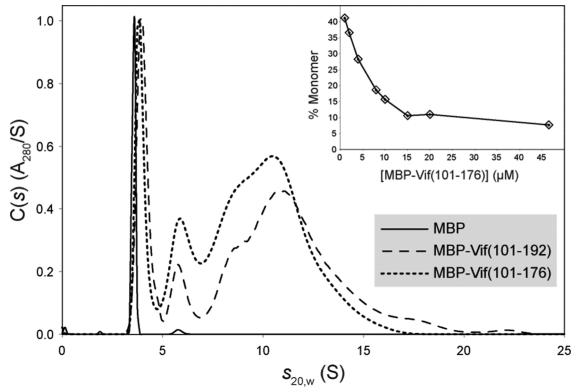

Figure 2. Sedimentation velocity analytical ultracentrifugation of MBP, MBP-Vif(101−192), and MBP-Vif(101−176). Proteins were concentrated to 10 μM. AUC data were analyzed as a continuous $c(s)$ distribution in SEDFIT as described in Materials and Methods. To compare the extent of oligomerization for each protein construct, the $c(s)$ plots were normalized to the area under the monomer peak. The inset shows the analysis of the reversibility of MBP-Vif(101−176) oligomerization. Protein samples were prepared by serial dilution of a 46.5 μM stock solution. AUC data were analyzed as described in Materials and Methods. The percent of monomeric Vif is plotted as a function of protein loading concentration.

modeling of the sedimentation velocity data in terms of a distribution of Lamm equation solutions. To account for boundary broadening due to diffusion, the analysis assumes that all of the sedimenting particles in the distribution have the same frictional ratio (f/f_o) that may not necessarily be the case. This value, used to relate the sedimentation coefficient and molecular mass, is predominantly determined by the major species.

The $c(s)$ profiles were integrated from 2.0 to 20.0 S to determine the fraction of protein present as a monomer. This analysis revealed that, at the standard loading concentration of 10 μM, <30% of MBP-Vif(101−176) and MBP-Vif(101−192) were present as monomers. To address the reversibility of Vif oligomerization, the fraction of monomeric MBP-Vif(101−176) was measured as a function of protein concentration. A stock solution of 46.5 μM MBP-Vif(101−176) was serially diluted and analyzed by sedimentation velocity AUC. The percent of monomeric species was determined by integrating the $c(s)$ profiles and is plotted as a function of protein concentration in the inset of Figure 2. The data show a precipitous drop in monomer content from 42 to 10% as the protein concentration was increased from 1 to 15 μM. Beyond 15 μM, there was little change in the percent of the monomer. Consistent with the percent of monomer data, the weight-average $s_{20,w}$ value, obtained by integrating the sedimentation $c(s)$ profile from 2.0 to 20.0 S, increased with an increasing protein concentration (data not shown). Because of the limits of detection provided by the absorbance and interference optics, we were unable to analyze protein samples at concentrations of <1 μM. However, even at 1 μM, a large fraction of Vif (58%) was still oligomeric. Overall, the data in the inset of Figure 2 demonstrate the reversibility of Vif oligomerization and illustrate its strong dependence on protein concentration.

Data presented in Figure 2 suggest that the last 16 residues of Vif (177−192) are not required for oligomerization. The MBP-Vif(101−176) fragment contains the HCCH motif, BC box, and PPLP motif. Because previous studies have focused on the

dx.doi.org/10.1021/bi201738a | *Biochemistry* 2012, 51, 2078−2086

PPLP motif as being essential for Vif oligomerization, we studied the oligomeric properties of MBP-Vif(154−176), which contains the PPLP motif but lacks both the HCCH motif and BC box. The $c(s)$ profile for MBP-Vif(154−176) (Figure 3)

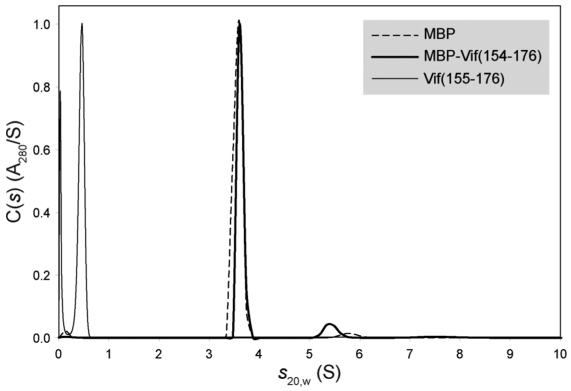

Figure 3. Sedimentation behavior of a Vif-PPLP peptide, free in solution or fused to MBP. Sedimentation velocity AUC data were analyzed as a continuous $c(s)$ distribution of sedimenting species. $c(s)$ profiles are shown for MBP (10 μM), MBP-Vif(154−176) (12 μM), and a synthetic PPLP peptide corresponding to Vif residues 155−176 (1.8 mM).

revealed that the protein was predominantly monomeric (>90% with $s_{20,w}$ = 3.7 S) with a small but significant amount of dimeric species ($s_{20,w}$ = 5.4 S). Because of the size of MBP, we wondered if the fusion tag could sterically hinder Vif oligomerization. A tag-free "PPLP peptide" (Vif residues 155−176), synthesized by solid phase peptide synthesis and purified by reversed phase HPLC, was therefore analyzed by sedimentation velocity AUC. At concentrations as high as 1.8 mM, the PPLP peptide sedimented as a single species with an $s_{20,w}$ of 0.45 S (Figure 3) and best-fit molecular mass of 2690 Da, which is (within the error of the method) identical to that calculated for the peptide monomer (2577 Da). As the value of the sedimentation coefficient does not change over the 10-fold concentration range studied, the data in Figure 3 strongly suggest that the PPLP peptide does not oligomerize. The data indicate that the PPLP motif alone is not sufficient to promote oligomerization of Vif and suggest the possibility that interaction with other upstream sequences (e.g., the BC box and HCCH motif) is required for oligomerization.

A small but significant amount of MBP-Vif(154−176) was dimeric (see the 5.4 S peak in Figure 3). MBP and MBP-Vif(154−176) were also analyzed by size exclusion chromatography. MBP eluted from the column as a narrow peak consistent with the monomer, while MBP-Vif(154−176) eluted as a broader peak, indicating the presence of higher-molecular mass species in addition to the major monomeric species (Figure S1 of the Supporting Information). It is possible that MBP induces a conformational change in the PPLP peptide that facilitates dimerization. The far-UV CD spectrum of the PPLP peptide revealed that it is largely unstructured in solution (Figure 4). Trifluoroethanol (TFE), a solvent well-known for its ability to induce structure in peptides and proteins,[65] was used to determine whether structural changes in the PPLP peptide could affect its oligomeric properties. Addition of TFE [20 or 40% (v/v)] to the PPLP peptide altered the far-UV CD spectrum, indicating a change in secondary structure (Figure 4). Data analysis revealed that the percentage of α-helical

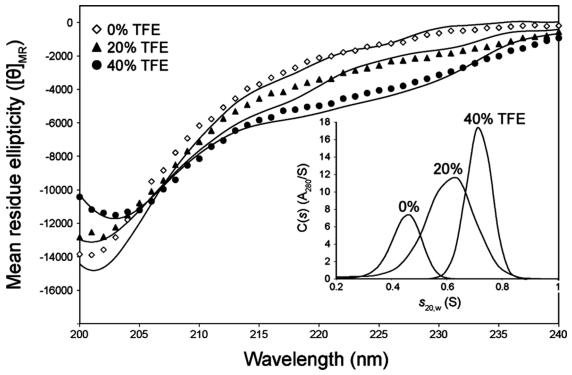

Figure 4. Trifluoroethanol-induced changes in the secondary structure and oligomeric properties of the Vif(155−176) peptide. Far-UV circular dichroism spectra of Vif(155−176) (final concentration of 48 μM) prepared in buffer containing 0, 20, or 40% (v/v) TFE. The inset shows $c(s)$ profiles for Vif(155−176) (final concentration of 140 μM) in the presence of 0, 20, or 40% TFE.

secondary structure in the PPLP peptide increased from 5% in buffer lacking TFE to 15% in a solution containing 40% TFE. Sedimentation velocity AUC experiments revealed that TFE induced oligomerization of the PPLP peptide (Figure 4, inset). The $c(s)$ profiles of the PPLP peptide prepared in increasing concentrations of TFE illustrate a clear trend from a monomeric form (0.45 S) in the absence of TFE to a higher-molecular mass form (0.75 S) in the presence of 40% TFE. As the interpretation of sedimentation velocity AUC data depends critically on solvent densities and viscosities, the $s_{20,w}$ values were corrected for the changes in solution viscosity and density caused by TFE using SEDNTERP. Ignoring possible contributions from hydration terms to the buoyant molecular mass and using a peptide partial specific volume calculated in SEDNTERP, we determine a best-fit molecular mass of 5210 Da for the 0.75 S species in 40% (v/v) TFE, consistent with a peptide dimer (M_{calc} = 5154 Da). As corrections for hydration contributions will lead to only larger true molecular masses, we conclude that the addition of TFE to the PPLP peptide induced a transition from a monomer to an oligomer (most likely dimer), suggesting that a modest change in the conformation of Vif residues 155−176 can promote oligomerization.

To identify other regions in the C-terminus of Vif required for oligomerization, we analyzed MBP-Vif(101−x) fragments (where x = 141, 153, 160, 165, or 172) by sedimentation velocity AUC. The $c(s)$ profiles for MBP-Vif(101−141) and MBP-Vif(101−153) revealed major sedimenting species with $s_{20,w}$ values of 3.6 and 3.8 S, respectively (Figure 5). Molecular masses for these species (42.7 and 43.6 kDa, respectively) indicate that these represent monomeric MBP-Vif(101−141) (M_{calc} = 46.1 kDa) and MBP-Vif(101−153) (M_{calc} = 47.3 kDa), respectively. In addition to the dominant monomeric species, oligomers of MBP-Vif(101−141) and MBP-Vif(101−153) were also observed (Figure 5). However, the extent of oligomerization observed for the Vif(101−141) and Vif(101−153) fragments was far less than what was observed for the Vif(101−176) fragment. Integration of the $c(s)$ profiles for the Vif(101−141) and Vif(101−153) fragments revealed that these proteins are ~60% monomeric compared to the Vif(101−176) fragment, which is 30% monomeric at the same loading concentration. Vif fragments longer than residues 101−153 (101−160, 101−165, and 101−172) were mostly oligomeric, forming a distribution of species with $s_{20,w}$ values ranging from 5

dx.doi.org/10.1021/bi201738a | Biochemistry 2012, 51, 2078−2086

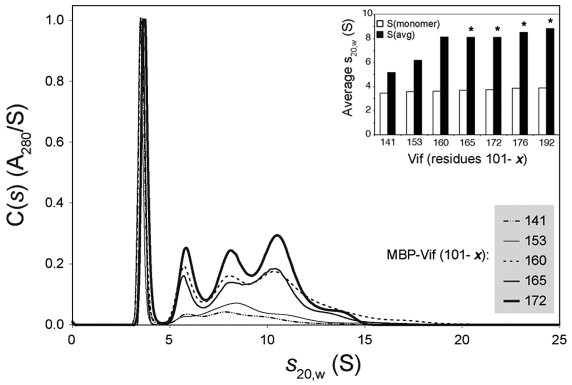

Figure 5. Oligomeric properties of Vif truncation mutants. Sedimentation velocity AUC experiments were conducted with MBP-Vif(101−x) fragments, where x = 141, 153, 160, 165, or 172. Proteins were purified as described and concentrated to 10 μM. AUC data were analyzed as described. For comparison, the $c(s)$ profiles were normalized according to the area under the monomer peak. The inset shows the weight-average $s_{20,w}$ values for MBP-Vif(101−x) constructs. Sedimentation velocity AUC analyses were performed using an equivalent concentration (final concentration of 10 μM) for all protein constructs. Weight-average $s_{20,w}$ values (filled bars) were calculated by integrating the $c(s)$ profiles from 2 to 20 S. Empty bars represent the $s_{20,w}$ value for the monomer species. Bars corresponding to constructs that contain the PPLP motif are marked with an asterisk.

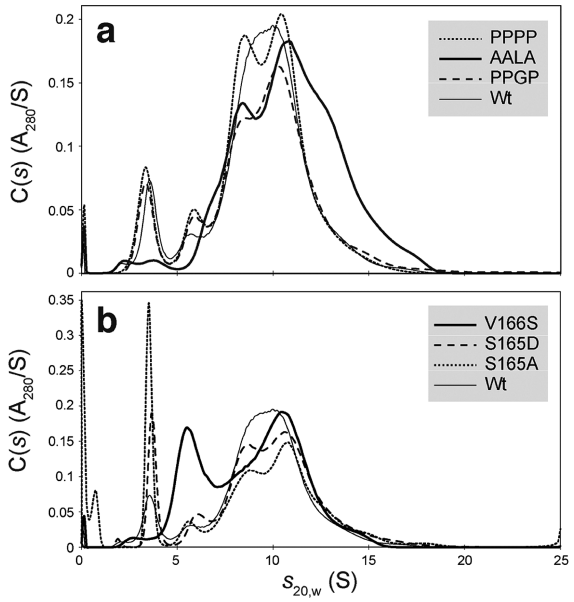

Figure 6. Oligomeric properties of Vif mutants. (a) Mutations in the PPLP motif (AALA, PPGP, and PPPP) were created in the MBP-Vif(101−176) construct, and purified proteins were concentrated to 30 μM. Proteins were analyzed by sedimentation velocity AUC. (b) Point mutations, S165A, S165D, and V166S, were created in the MBP-Vif(101−176) construct, and purified proteins were concentrated to 30 μM. Sedimentation velocity AUC data were analyzed as described in Materials and Methods.

to 20 S (Figure 5). In these cases, <30% of the protein was monomeric, comparable to the case for the Vif(101−176) fragment.

The weight-average $s_{20,w}$ value, obtained by integrating the $c(s)$ profile from 2.0 to 20.0 S, was calculated for each MBP-Vif construct (filled bars in the inset of Figure 5). This value was compared to the monomer $s_{20,w}$ value for each construct (empty bars). The monomer $s_{20,w}$ values increase as expected for the changes in the size of the Vif fragments. Comparison of the weight-average $s_{20,w}$ values reveals that the most significant increase in oligomeric species was due to residues 154−160 (compare the weight-average $s_{20,w}$ values for fragments of residues 101−153 and 101−160 of Vif). Addition of residues 161−165 that encompass the PPLP motif did not cause an increase in the weight-average $s_{20,w}$ value, further emphasizing the fact that the PPLP motif is not essential for Vif oligomerization.

Mutations were engineered into and surrounding the PPLP motif in MBP-Vif(101−176), and the effects on oligomerization were determined by sedimentation velocity AUC. We mutated the PPLP motif to AALA in the backbone of the MBP-Vif(101−176) construct to determine the role of the conserved proline residues in oligomerization. Inspection of the $c(s)$ profile of MBP-Vif(101−176)$_{AALA}$ revealed that this mutant contained much less of the monomeric form and more oligomers than the wild-type construct (Figure 6a). Two other PPLP mutants were analyzed, namely, PPLP → PPGP (L163G) and PPLP → PPPP (L163P). MBP-Vif(101−176)$_{PPGP}$ and MBP-Vif(101−176)$_{PPPP}$ also formed oligomers (Figure 6a), demonstrating that mutation of the PPLP motif does not abolish oligomerization. The data support the idea that the PPLP motif is not required for oligomerization. Instead, the PPLP motif may orient surrounding residues that make contacts in the oligomer.

Two highly conserved residues near the PPLP motif, V166 and S165, were mutated in MBP-Vif(101−176) to determine their role in Vif oligomerization. Mutation of V166 to S caused a dramatic reduction in the amount of monomer and an increase in the amount of dimer (Figure 6b). This effect can be seen in the monomeric region of the $c(s)$ profiles ($s_{20,w}$ = 3.6−4 S) where the amount of monomer detected for the V166S mutant was significantly smaller than the amount in wild-type Vif. In addition, the $s_{20,w}$ peak at 6 S (corresponding to the dimer) was much more pronounced for the V166S mutant. Comparison of the $c(s)$ profiles for the S165D and S165A mutants revealed that these mutations stabilized the monomeric form of MBP-Vif(101−176) (Figure 6b). This effect can be seen in the monomeric region of the $c(s)$ profiles ($s_{20,w}$ = 3.6−4 S). The increase in the amount of monomeric species for the S165D and S165A mutants was balanced by a decrease in the amount of oligomers ($s_{20,w}$ = 7.0−15 S). Notably, the amount of dimer ($s_{20,w}$ = 6 S) was very similar between wild-type Vif and the S165 mutants (Figure 6b).

The V166S, S165D, and S165A mutations were generated in full-length Vif to determine their impact on the ability of Vif to degrade APOBEC3G. Vif-dependent degradation of APOBEC3G was measured by immunoblotting.[66] Vif and APOBEC3G were transiently expressed in HeLa cells, separated by SDS−PAGE, and subjected to immunoblot analysis using antibodies to APOBEC3G, Vif, and tubulin (as a loading control). The APOBEC3G degradation data (Figure 7a) indicate that the S165D and V166S Vif mutants were unable to efficiently degrade APOBEC3G and were comparable to the control lacking Vif. The APOBEC3G degradation activity of the S165A mutant was comparable to that of wild-type Vif. The ability of the Vif mutants to interact with APOBEC3G was tested by co-immunoprecipitation (Materials and Methods) (Figure 7b,c). To prevent Vif-induced APOBEC3G degradation in this experiment, a dominant-

dx.doi.org/10.1021/bi201738a | Biochemistry 2012, 51, 2078−2086

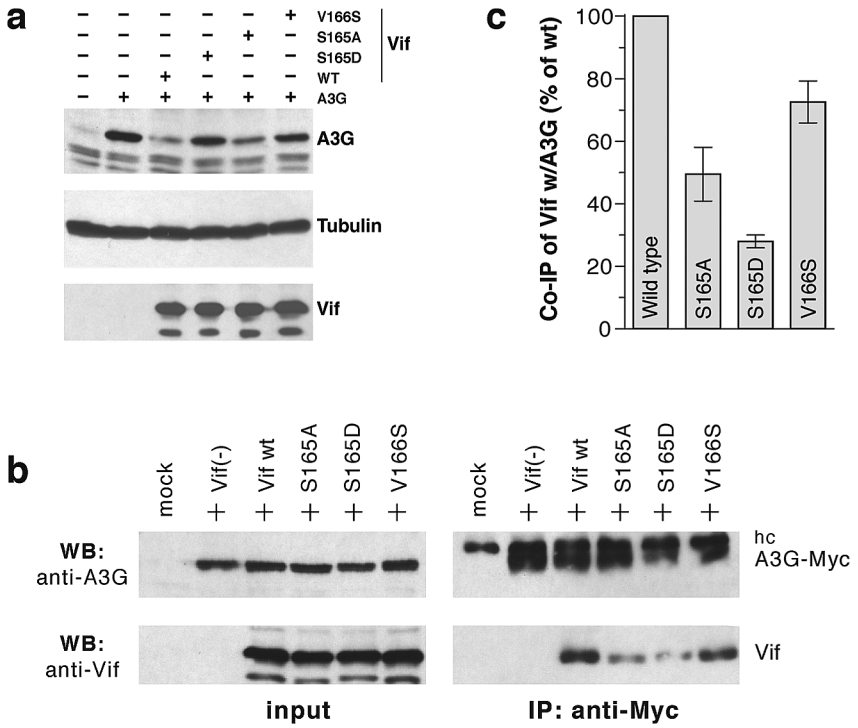

Figure 7. Functional analysis of S165 and V166 mutants of Vif. (a) Vif-induced degradation of APOBEC3G. HeLa cells transiently expressing Vif and APOBEC3G were harvested and probed using antibodies to APOBEC3G or Vif. (b) Co-immunoprecipitation of Vif and APOBEC3G. HeLa cells were transfected with vectors encoding Vif, APOBEC3G-Myc, and Cul5ΔRbx. Cul5ΔRbx was included to prohibit Vif-induced degradation of A3G in this experiment.[21] Anti-Myc immunoprecipitates were separated by SDS−PAGE and probed with antibodies to Vif and Myc (right). Total cell extracts served as input control and were used to correct for fluctuations in Vif expression levels (left). (c) Results from three independent experiments were quantified. The amount of coprecipitated wt Vif is defined as 100%, and the amount of coprecipitated mutant Vif protein is expressed as a percentage of that of wt Vif.

negative form of Cul5 (Cul5ΔRbx) was cotransfected. The results demonstrate that all of the mutations weakened the Vif−APOBEC3G interaction irrespective of the functional phenotype. This suggests that mutations in Vif that affect interaction with APOBEC3G are not necessarily indicative of the effects of Vif on APOBEC3G degradation. Nevertheless, the data in Figures 6 and 7 reveal that the same residues involved in oligomerization are also important for APOBEC3G binding and degradation.

DISCUSSION

This represents the first detailed hydrodynamic analysis of HIV-1 Vif oligomerization using AUC. A major finding of this study is that the PPLP motif is not essential for Vif oligomerization. Previous studies have suggested that the PPLP motif is essential for oligomerization.[51,52] These studies utilized an assay in which immobilized GST-bound Vif was used to pull down ^{35}S-labeled Vif. Our AUC studies are fundamentally different from these earlier studies because they are performed in solution. It is possible that the conformation of GST-bound Vif attached to the solid surface is different from the conformation in solution. Recently, AUC analysis of Vif(139−176), which contains the BC box and PPLP motif, revealed that this fragment of Vif is monomeric.[46] Dynamic light scattering was used to examine the impact of the AALA mutation on Vif oligomerization.[61] The authors found that this mutation reduced but did not abolish oligomerization. AUC revealed that the AALA mutation abolished monomeric Vif and stabilized higher-order oligomers (Figure 6a). Mutation of the PPLP motif to the AALA motif may create a hydrophobic patch that stabilizes oligomeric forms of Vif. However, because the PPLP sequence is likely to impose very unique constraints on the conformation of Vif, indirect effects on oligomerization caused by the AALA mutation cannot be ruled out. Although the PPLP motif is clearly important for Vif function, our data and the studies mentioned support our assertion that the PPLP motif is not essential for oligomerization.

Our data suggest that the mechanism of oligomerization is more complex than previously thought. The HCCH motif appears to be involved in oligomerization. The $c(s)$ profile of MBP-Vif(101−141) revealed the presence of oligomers (Figure 5), and the weight-average $s_{20,w}$ value for this construct was significantly greater than that for the monomer (Figure 5, inset). It is important to emphasize that these studies were performed in the absence of zinc, which is known to alter the conformation of the HCCH motif.[42,67] Addition of zinc to MBP-Vif(101−176) altered its oligomeric properties, and this effect could be reversed by the addition of EDTA (Figure S2 of the Supporting Information), further suggesting that Vif oligomerization is sensitive to the conformation of the HCCH motif. The BC box may also be involved in oligomerization. MBP-Vif(101−153), which includes the HCCH motif and BC box, oligomerized to a greater extent than MBP-Vif(101−141). This can be seen by comparing the $c(s)$ profiles for these constructs (Figure 5) as well as their weight-average $s_{20,w}$ values (Figure 5, inset). Tween 20 [0.05% (v/v)] did not alter the $c(s)$ profile for MBP-Vif(101−153) (data not shown), suggesting that oligomerization is mediated by specific protein−protein interactions. Even the subtle mutation of L145 to A in the BC box significantly altered the

dx.doi.org/10.1021/bi201738a | *Biochemistry* 2012, 51, 2078−2086

oligomeric properties of MBP-Vif(101−176) (Figure S3 of the Supporting Information). Thus, we favor a mechanism in which the HCCH motif, BC box, and PPLP motif interact to generate a conformation that promotes oligomerization.

Our studies highlight the biochemical and conformational properties of the PPLP peptide corresponding to Vif residues 155−176. This peptide lacked strong secondary structure. Interestingly, TFE induced α-helical secondary structure in this peptide (Figure 4) and promoted peptide oligomerization (inset of Figure 4). In the absence of TFE, the peptide was monomeric even at a concentration as high as 1.8 mM. However, when the PPLP peptide was fused to the C-terminus of MBP, which is normally monomeric, a significant amount of the fusion protein formed dimers (Figure 3). Experiments using NMR[46] and hydrogen exchange mass spectrometry[50] suggest that the region containing the PPLP motif is highly dynamic. The fact that the PPLP peptide was monomeric unless fused to MBP or MBP-Vif constructs [e.g., MBP-Vif(101−176)] suggests that this region of Vif may undergo induced folding to generate a conformation that promotes oligomerization. A similar induced-folding mechanism has been proposed to explain the interaction of the region containing the BC box and PPLP motif with elongin B/C.[46,50]

Residues immediately upstream from the PPLP motif (I^{154}TPKKIK^{160}) were most critical for oligomerization. This can seen by comparing the weight-average $s_{20,w}$ values for MBP-Vif fragments 101−153, 101−160, and 101−165 (Figure 5, inset). However, mutation of the PPLP motif (Figure 6a) or residues immediately downstream from the PPLP motif (Figure 6b) also perturbed the oligomeric properties of Vif. Mutation of V166 to S greatly affected the oligomeric properties of Vif, by destabilizing the monomeric form and stabilizing the dimeric form relative to the wild-type protein, which can be seen from the $c(s)$ profiles in Figure 6b. The oligomeric properties of Vif were sensitive to mutations at position 165. Replacement of serine at this position with either alanine or aspartate stabilized the monomeric form of Vif and destabilized higher-order oligomeric forms (Figure 6b). S165 is highly conserved among HIV-1 Vif sequences and is thought to be targeted for phosphorylation by MAPK.[68] Phosphorylation of S165 could provide a mechanism for modulating the conformation and oligomeric properties of Vif in vivo.

We tested the functional impact of the S165 and V166 mutations by determining the ability of the mutant Vif proteins to degrade APOBEC3G (Figure 7a). The effect of the mutations can be ranked according to severity as follows: V166S > S165D > S165A > wild-type Vif. The effect of these mutations on the oligomeric properties of Vif follows a similar trend (Figure 6b). Interestingly, all the mutants were defective in their ability to interact with APOBEC3G (Figure 7b,c), suggesting that the C-terminus of HIV-1 Vif plays an important role in binding APOBEC3G. This effect could be direct or could be the result of misfolding caused by the mutations.

What we have learned is that oligomerization of HIV-1 Vif requires a region in the C-terminus that encompasses the HCCH motif, BC box, and PPLP motif. The exact role of the PPLP motif in Vif function remains unclear, but we propose that its main role is to properly orient nearby residues that mediate protein−protein interactions. Vif is a dynamic protein, and this conformational complexity may be essential for mediation of many different protein interactions like Cul5 binding, elongin B/C binding, Vif−Vif binding, and APOBEC3G binding. With regard to the oligomeric state of Vif, several oligomeric forms have been identified here and in other studies.[44,51,61] Our results indicate that mutations that affect Vif oligomerization also affect the ability to bind and degrade APOBEC3G. One explanation is that a common surface in Vif mediates oligomerization and APOBEC3G binding. It is also possible that Vif oligomerization facilitates APOBEC3G binding. In the cell, APOBEC3G exists in a high-molecular mass form that is stabilized by RNA.[69] Vif oligomers may be able to more avidly bind to the high-molecular mass form of APOBEC3G. On the other hand, a recent study found that Vif−elongin B/C−Cul5 complexes contain monomeric Vif.[44] Ultimately, the role of Vif is to exclude APOBEC3G from budding viral particles. Vif monomers may function to recruit the Cul5 ubiquitin ligase machinery and induce the degradation of APOBEC3G. Vif oligomers could stabilize high-molecular mass APOBEC3G complexes and prevent viral packaging of APOBEC3G by a degradation-independent pathway. Further studies are required to understand how Vif oligomerization affects its interactions with APOBEC3G as well as other binding partners.

■ ASSOCIATED CONTENT

Supporting Information

Size exclusion analysis of MBP-Vif(154−176) and supporting sedimentation velocity data for MBP-Vif(101−176). This material is available free of charge via the Internet at http://pubs.acs.org.

■ AUTHOR INFORMATION

Corresponding Author

*E-mail: emaynard@usuhs.mil. Telephone: (301) 295-2845. Fax: (301) 295-3512.

Funding

This work was supported by the Edward Mallinckrodt Jr. Foundation (E.L.M. and S.M.T.), the National Institutes of Health Intramural Research Programs of the National Institute of Allergy and Infectious Diseases (K.S. and S.K.), and the National Institute of Diabetes and Digestive and Kidney Diseases (R.G.).

Notes

The authors declare no competing financial interest.

■ ACKNOWLEDGMENTS

We thank Sudipa Ghimire and Kalyan Giri for careful review of the manuscript.

■ ABBREVIATIONS

APOBEC3G, apolipoprotein B mRNA-editing enzyme catalytic polypeptide-like 3G; AUC, analytical ultracentrifugation; CD, circular dichroism; PPLP peptide, Vif residues 155−176; RING, really interesting new gene; SOCS, suppressor of cytokine signaling; Vif, virion infectivity factor.

■ REFERENCES

(1) Sheehy, A. M., Gaddis, N. C., Choi, J. D., and Malim, M. H. (2002) Isolation of a human gene that inhibits HIV-1 infection and is suppressed by the viral Vif protein. *Nature 418*, 646−650.

(2) Bishop, K. N., Holmes, R. K., Sheehy, A. M., Davidson, N. O., Cho, S. J., and Malim, M. H. (2004) Cytidine deamination of retroviral DNA by diverse APOBEC proteins. *Curr. Biol. 14*, 1392−1396.

(3) Liddament, M. T., Brown, W. L., Schumacher, A. J., and Harris, R. S. (2004) APOBEC3F properties and hypermutation preferences indicate activity against HIV-1 in vivo. *Curr. Biol. 14*, 1385−1391.

(4) Wiegand, H. L., Doehle, B. P., Bogerd, H. P., and Cullen, B. R. (2004) A second human antiretroviral factor, APOBEC3F, is suppressed by the HIV-1 and HIV-2 Vif proteins. *EMBO J. 23*, 2451−2458.
(5) Zheng, Y. H., Irwin, D., Kurosu, T., Tokunaga, K., Sata, T., and Peterlin, B. M. (2004) Human APOBEC3F is another host factor that blocks human immunodeficiency virus type 1 replication. *J. Virol. 78*, 6073−6076.
(6) Luo, K., Liu, B., Xiao, Z., Yu, Y., Yu, X., Gorelick, R., and Yu, X. F. (2004) Amino-terminal region of the human immunodeficiency virus type 1 nucleocapsid is required for human APOBEC3G packaging. *J. Virol. 78*, 11841−11852.
(7) Cen, S., Guo, F., Niu, M., Saadatmand, J., Deflassieux, J., and Kleiman, L. (2004) The interaction between HIV-1 Gag and APOBEC3G. *J. Biol. Chem. 279*, 33177−33184.
(8) Alce, T. M., and Popik, W. (2004) APOBEC3G is incorporated into virus-like particles by a direct interaction with HIV-1 Gag nucleocapsid protein. *J. Biol. Chem. 279*, 34083−34086.
(9) Douaisi, M., Dussart, S., Courcoul, M., Bessou, G., Vigne, R., and Decroly, E. (2004) HIV-1 and MLV Gag proteins are sufficient to recruit APOBEC3G into virus-like particles. *Biochem. Biophys. Res. Commun. 321*, 566−573.
(10) Schafer, A., Bogerd, H. P., and Cullen, B. R. (2004) Specific packaging of APOBEC3G into HIV-1 virions is mediated by the nucleocapsid domain of the gag polyprotein precursor. *Virology 328*, 163−168.
(11) Svarovskaia, E. S., Xu, H., Mbisa, J. L., Barr, R., Gorelick, R. J., Ono, A., Freed, E. O., Hu, W. S., and Pathak, V. K. (2004) Human apolipoprotein B mRNA-editing enzyme-catalytic polypeptide-like 3G (APOBEC3G) is incorporated into HIV-1 virions through interactions with viral and nonviral RNAs. *J. Biol. Chem. 279*, 35822−35828.
(12) Zennou, V., Perez-Caballero, D., Gottlinger, H., and Bieniasz, P. D. (2004) APOBEC3G incorporation into human immunodeficiency virus type 1 particles. *J. Virol. 78*, 12058−12061.
(13) Khan, M. A., Kao, S., Miyagi, E., Takeuchi, H., Goila-Gaur, R., Opi, S., Gipson, C. L., Parslow, T. G., Ly, H., and Strebel, K. (2005) Viral RNA is required for the association of APOBEC3G with human immunodeficiency virus type 1 nucleoprotein complexes. *J. Virol. 79*, 5870−5874.
(14) Navarro, F., Bollman, B., Chen, H., Konig, R., Yu, Q., Chiles, K., and Landau, N. R. (2005) Complementary function of the two catalytic domains of APOBEC3G. *Virology 333*, 374−386.
(15) Burnett, A., and Spearman, P. (2007) APOBEC3G multimers are recruited to the plasma membrane for packaging into human immunodeficiency virus type 1 virus-like particles in an RNA-dependent process requiring the NC basic linker. *J. Virol. 81*, 5000−5013.
(16) Harris, R. S., Bishop, K. N., Sheehy, A. M., Craig, H. M., Petersen-Mahrt, S. K., Watt, I. N., Neuberger, M. S., and Malim, M. H. (2003) DNA deamination mediates innate immunity to retroviral infection. *Cell 113*, 803−809.
(17) Lecossier, D., Bouchonnet, F., Clavel, F., and Hance, A. J. (2003) Hypermutation of HIV-1 DNA in the absence of the Vif protein. *Science 300*, 1112.
(18) Mangeat, B., Turelli, P., Caron, G., Friedli, M., Perrin, L., and Trono, D. (2003) Broad antiretroviral defence by human APOBEC3G through lethal editing of nascent reverse transcripts. *Nature 424*, 99−103.
(19) Mariani, R., Chen, D., Schrofelbauer, B., Navarro, F., Konig, R., Bollman, B., Munk, C., Nymark-McMahon, H., and Landau, N. R. (2003) Species-specific exclusion of APOBEC3G from HIV-1 virions by Vif. *Cell 114*, 21−31.
(20) Zhang, H., Yang, B., Pomerantz, R. J., Zhang, C., Arunachalam, S. C., and Gao, L. (2003) The cytidine deaminase CEM15 induces hypermutation in newly synthesized HIV-1 DNA. *Nature 424*, 94−98.
(21) Yu, X., Yu, Y., Liu, B., Luo, K., Kong, W., Mao, P., and Yu, X. F. (2003) Induction of APOBEC3G ubiquitination and degradation by an HIV-1 Vif-Cul5-SCF complex. *Science 302*, 1056−1060.
(22) Jager, S., Kim, D. Y., Hultquist, J. F., Shindo, K., LaRue, R. S., Kwon, E., Li, M., Anderson, B. D., Yen, L., Stanley, D., Mahon, C., Kane, J., Franks-Skiba, K., Cimermancic, P., Burlingame, A., Sali, A., Craik, C. S., Harris, R. S., Gross, J. D., and Krogan, N. J. (2012) Vif hijacks CBF-β to degrade APOBEC3G and promote HIV-1 infection. *Nature 481*, 371−375.
(23) Zhang, W., Du, J., Evans, S. L., Yu, Y., and Yu, X. F. (2012) T-cell differentiation factor CBF-β regulates HIV-1 Vif-mediated evasion of host restriction. *Nature 481*, 376−379.
(24) Conticello, S. G., Harris, R. S., and Neuberger, M. S. (2003) The Vif protein of HIV triggers degradation of the human antiretroviral DNA deaminase APOBEC3G. *Curr. Biol. 13*, 2009−2013.
(25) Kobayashi, M., Takaori-Kondo, A., Miyauchi, Y., Iwai, K., and Uchiyama, T. (2005) Ubiquitination of APOBEC3G by an HIV-1 Vif-Cullin5-Elongin B-Elongin C complex is essential for Vif function. *J. Biol. Chem. 280*, 18573−18578.
(26) Marin, M., Rose, K. M., Kozak, S. L., and Kabat, D. (2003) HIV-1 Vif protein binds the editing enzyme APOBEC3G and induces its degradation. *Nat. Med. 9*, 1398−1403.
(27) Mehle, A., Strack, B., Ancuta, P., Zhang, C., McPike, M., and Gabuzda, D. (2004) Vif overcomes the innate antiviral activity of APOBEC3G by promoting its degradation in the ubiquitin-proteasome pathway. *J. Biol. Chem. 279*, 7792−7798.
(28) Stopak, K., de Noronha, C., Yonemoto, W., and Greene, W. C. (2003) HIV-1 Vif blocks the antiviral activity of APOBEC3G by impairing both its translation and intracellular stability. *Mol. Cell 12*, 591−601.
(29) Chen, G., He, Z., Wang, T., Xu, R., and Yu, X. F. (2009) A patch of positively charged amino acids surrounding the human immunodeficiency virus type 1 Vif SLVx4Yx9Y motif influences its interaction with APOBEC3G. *J. Virol. 83*, 8674−8682.
(30) Dang, Y., Davis, R. W., York, I. A., and Zheng, Y. H. (2010) Identification of 81LGxGxxIxW89 and 171EDRW174 domains from human immunodeficiency virus type 1 Vif that regulate APOBEC3G and APOBEC3F neutralizing activity. *J. Virol. 84*, 5741−5750.
(31) Dang, Y., Wang, X., Zhou, T., York, I. A., and Zheng, Y. H. (2009) Identification of a novel WxSLVK motif in the N terminus of human immunodeficiency virus and simian immunodeficiency virus Vif that is critical for APOBEC3G and APOBEC3F neutralization. *J. Virol. 83*, 8544−8552.
(32) He, Z., Zhang, W., Chen, G., Xu, R., and Yu, X. F. (2008) Characterization of conserved motifs in HIV-1 Vif required for APOBEC3G and APOBEC3F interaction. *J. Mol. Biol. 381*, 1000−1011.
(33) Pery, E., Rajendran, K. S., Brazier, A. J., and Gabuzda, D. (2009) Regulation of APOBEC3 proteins by a novel YXXL motif in human immunodeficiency virus type 1 Vif and simian immunodeficiency virus SIVagm Vif. *J. Virol. 83*, 2374−2381.
(34) Russell, R. A., and Pathak, V. K. (2007) Identification of two distinct human immunodeficiency virus type 1 Vif determinants critical for interactions with human APOBEC3G and APOBEC3F. *J. Virol. 81*, 8201−8210.
(35) Schrofelbauer, B., Senger, T., Manning, G., and Landau, N. R. (2006) Mutational alteration of human immunodeficiency virus type 1 Vif allows for functional interaction with nonhuman primate APOBEC3G. *J. Virol. 80*, 5984−5991.
(36) Mehle, A., Goncalves, J., Santa-Marta, M., McPike, M., and Gabuzda, D. (2004) Phosphorylation of a novel SOCS-box regulates assembly of the HIV-1 Vif-Cul5 complex that promotes APOBEC3G degradation. *Genes Dev. 18*, 2861−2866.
(37) Yu, Y., Xiao, Z., Ehrlich, E. S., Yu, X., and Yu, X. F. (2004) Selective assembly of HIV-1 Vif-Cul5-ElonginB-ElonginC E3 ubiquitin ligase complex through a novel SOCS box and upstream cysteines. *Genes Dev. 18*, 2867−2872.
(38) Luo, K., Xiao, Z., Ehrlich, E., Yu, Y., Liu, B., Zheng, S., and Yu, X. F. (2005) Primate lentiviral virion infectivity factors are substrate receptors that assemble with cullin 5-E3 ligase through a HCCH motif to suppress APOBEC3G. *Proc. Natl. Acad. Sci. U.S.A. 102*, 11444−11449.

(39) Mehle, A., Thomas, E. R., Rajendran, K. S., and Gabuzda, D. (2006) A zinc-binding region in Vif binds Cul5 and determines cullin selection. *J. Biol. Chem. 281*, 17259−17265.
(40) Xiao, Z., Ehrlich, E., Yu, Y., Luo, K., Wang, T., Tian, C., and Yu, X. F. (2006) Assembly of HIV-1 Vif-Cul5 E3 ubiquitin ligase through a novel zinc-binding domain-stabilized hydrophobic interface in Vif. *Virology 349*, 290−299.
(41) Giri, K., Scott, R. A., and Maynard, E. L. (2009) Molecular Structure and Biochemical Properties of the HCCH-Zn^{2+} Site in HIV-1 Vif. *Biochemistry 48*, 7969−7978.
(42) Paul, I., Cui, J., and Maynard, E. L. (2006) Zinc binding to the HCCH motif of HIV-1 virion infectivity factor induces a conformational change that mediates protein-protein interactions. *Proc. Natl. Acad. Sci. U.S.A. 103*, 18475−18480.
(43) Stanley, B. J., Ehrlich, E. S., Short, L., Yu, Y., Xiao, Z., Yu, X. F., and Xiong, Y. (2008) Structural Insight into the HIV Vif SOCS Box and Its Role in Human E3 Ubiquitin Ligase Assembly. *J. Virol. 82*, 8656−8663.
(44) Wolfe, L. S., Stanley, B. J., Liu, C., Eliason, W. K., and Xiong, Y. (2010) Dissection of HIV Vif interaction with the human E3 ubiquitin ligase. *J. Virol. 84*, 7135−7139.
(45) Kamura, T., Maenaka, K., Kotoshiba, S., Matsumoto, M., Kohda, D., Conaway, R. C., Conaway, J. W., and Nakayama, K. I. (2004) VHL-box and SOCS-box domains determine binding specificity for Cul2-Rbx1 and Cul5-Rbx2 modules of ubiquitin ligases. *Genes Dev. 18*, 3055−3065.
(46) Bergeron, J. R., Huthoff, H., Veselkov, D. A., Beavil, R. L., Simpson, P. J., Matthews, S. J., Malim, M. H., and Sanderson, M. R. (2010) The SOCS-box of HIV-1 Vif interacts with ElonginBC by induced-folding to recruit its Cul5-containing ubiquitin ligase complex. *PLoS Pathog. 6*, e1000925.
(47) Donahue, J. P., Vetter, M. L., Mukhtar, N. A., and D'Aquila, R. T. (2008) The HIV-1 Vif PPLP motif is necessary for human APOBEC3G binding and degradation. *Virology 377*, 49−53.
(48) Walker, R. C. Jr., Khan, M. A., Kao, S., Goila-Gaur, R., Miyagi, E., and Strebel, K. (2010) Identification of dominant negative human immunodeficiency virus type 1 Vif mutants that interfere with the functional inactivation of APOBEC3G by virus-encoded Vif. *J. Virol. 84*, 5201−5211.
(49) Auclair, J. R., Green, K. M., Shandilya, S., Evans, J. E., Somasundaran, M., and Schiffer, C. A. (2007) Mass spectrometry analysis of HIV-1 Vif reveals an increase in ordered structure upon oligomerization in regions necessary for viral infectivity. *Proteins 69*, 270−284.
(50) Marcsisin, S. R., and Engen, J. R. (2010) Molecular insight into the conformational dynamics of the Elongin BC complex and its interaction with HIV-1 Vif. *J. Mol. Biol. 402*, 892−904.
(51) Yang, S., Sun, Y., and Zhang, H. (2001) The multimerization of human immunodeficiency virus type I Vif protein: A requirement for Vif function in the viral life cycle. *J. Biol. Chem. 276*, 4889−4893.
(52) Yang, B., Gao, L., Li, L., Lu, Z., Fan, X., Patel, C. A., Pomerantz, R. J., DuBois, G. C., and Zhang, H. (2003) Potent suppression of viral infectivity by the peptides that inhibit multimerization of human immunodeficiency virus type 1 (HIV-1) Vif proteins. *J. Biol. Chem. 278*, 6596−6602.
(53) Miller, J. H., Presnyak, V., and Smith, H. C. (2007) The dimerization domain of HIV-1 viral infectivity factor Vif is required to block virion incorporation of APOBEC3G. *Retrovirology 4*, 81.
(54) Pace, C. N., Vajdos, F., Fee, L., Grimsley, G., and Gray, T. (1995) How to measure and predict the molar absorption coefficient of a protein. *Protein Sci. 4*, 2411−2423.
(55) Schuck, P. (2000) Size-distribution analysis of macromolecules by sedimentation velocity ultracentrifugation and Lamm equation modeling. *Biophys. J. 78*, 1606−1619.
(56) Cole, J. L., Lary, J. W., P Moody, T., and Laue, T. M. (2008) Analytical ultracentrifugation: Sedimentation velocity and sedimentation equilibrium. *Methods Cell Biol. 84*, 143−179.
(57) Provencher, S. W., and Glockner, J. (1981) Estimation of globular protein secondary structure from circular dichroism. *Biochemistry 20*, 33−37.
(58) Lees, J. G., Smith, B. R., Wien, F., Miles, A. J., and Wallace, B. A. (2004) CDtool: An integrated software package for circular dichroism spectroscopic data processing, analysis, and archiving. *Anal. Biochem. 332*, 285−289.
(59) Lobley, A., Whitmore, L., and Wallace, B. A. (2002) DICHROWEB: An interactive website for the analysis of protein secondary structure from circular dichroism spectra. *Bioinformatics 18*, 211−212.
(60) Whitmore, L., and Wallace, B. A. (2004) DICHROWEB, an online server for protein secondary structure analyses from circular dichroism spectroscopic data. *Nucleic Acids Res. 32*, W668−W673.
(61) Bernacchi, S., Mercenne, G., Tournaire, C., Marquet, R., and Paillart, J. C. (2011) Importance of the proline-rich multimerization domain on the oligomerization and nucleic acid binding properties of HIV-1 Vif. *Nucleic Acids Res. 39*, 2404−2415.
(62) Henriet, S., Richer, D., Bernacchi, S., Decroly, E., Vigne, R., Ehresmann, B., Ehresmann, C., Paillart, J. C., and Marquet, R. (2005) Cooperative and specific binding of Vif to the 5′ region of HIV-1 genomic RNA. *J. Mol. Biol. 354*, 55−72.
(63) Bernacchi, S., Henriet, S., Dumas, P., Paillart, J. C., and Marquet, R. (2007) RNA and DNA binding properties of HIV-1 Vif protein: A fluorescence study. *J. Biol. Chem. 282*, 26361−26368.
(64) Zhao, H., Brown, P. H., Balbo, A., Fernandez-Alonso Mdel, C., Polishchuck, N., Chaudhry, C., Mayer, M. L., Ghirlando, R., and Schuck, P. (2010) Accounting for solvent signal offsets in the analysis of interferometric sedimentation velocity data. *Macromol. Biosci. 10*, 736−745.
(65) Buck, M. (1998) Trifluoroethanol and colleagues: Cosolvents come of age. Recent studies with peptides and proteins. *Q. Rev. Biophys. 31*, 297−355.
(66) Kao, S., Goila-Gaur, R., Miyagi, E., Khan, M. A., Opi, S., Takeuchi, H., and Strebel, K. (2007) Production of infectious virus and degradation of APOBEC3G are separable functional properties of human immunodeficiency virus type 1 Vif. *Virology 369*, 329−339.
(67) Giri, K., and Maynard, E. L. (2009) Conformational analysis of a peptide approximating the HCCH motif in HIV-1 Vif. *Pept. Sci. 92*, 417−425.
(68) Yang, X., Goncalves, J., and Gabuzda, D. (1996) Phosphorylation of Vif and its role in HIV-1 replication. *J. Biol. Chem. 271*, 10121−10129.
(69) Chiu, Y. L., Soros, V. B., Kreisberg, J. F., Stopak, K., Yonemoto, W., and Greene, W. C. (2005) Cellular APOBEC3G restricts HIV-1 infection in resting CD4+ T cells. *Nature 435*, 108−114.